AUTOMATED IMAGE ANALYSIS CHARACTERIZATION OF OXIDATION PROFILES AND POROSITY DEVELOPMENT DURING AIR OXIDATION OF NUCLEAR GRAPHITE

Cristian I. Contescu and Timothy D. Burchell

Oak Ridge National Laboratory, P.O.Box 2008, MS-6087
1 Bethel Valley Road, Oak Ridge, TN 37831, USA

Introduction

The Next Generation Nuclear Plant (NGNP) will be a high temperature gas-cooled reactor (HTGR) of modular construction, with the moderator and core components consisting mainly of graphite. Because of the limited oxidation stability of graphite at high temperatures, it is particularly important to understand the mechanism of porosity development in the oxidized layer and the effect of oxidation on mechanical properties. Along with other physical methods for characterization of density gradients in oxidized graphite materials [1,2], optical microscopy coupled with automated image analysis is a powerful and convenient technique for studying porosity development during oxidation of graphite.

Experimental

A sample of purified, nuclear-grade graphite material was chosen for oxidation tests. Cylindrical shaped specimens (25.4 mm x 25.4 mm diameter) were machined using only carbide cutting tools. The specimens were oxidized in air according to recommendations of ASTM D-7542-09. Three temperatures (600, 650, and 750 ^{o}C) and four levels of weight loss (5 to 20 %) were selected at each temperature. Oxidized specimens were cut transversally, mounted in resin, and polished for examination by optical microscopy. A Nikon Microphot FXA microscope with motorized stage and autofocus control was used. Several hundred optical micrographs were recorded using Leica Application Suite software. All images were recorded on monochromatic 8-bit grey scale, where pixel intensities vary between 0 for total black and 255 for absolute white. Individual images were stitched together into a rectangular mosaic image (25.4 x 4 mm) extending along the diameter of each specimen.

Mosaic images were processed using ImagePro software. In the pre-analysis stage, the image quality was improved by correcting excessive contrast, lightness or darkness. This stage also included spatial calibration against a reference scale. In the second stage, the software was instructed to recognize objects in the image (i.e. graphite pores) and to interpret the information. This operation is based on analysis of grey scale intensities in the pixel histogram of each image. The histogram provides the frequency of pixel values distribution on a scale from 0 (black) to 255 (white). The reflective surface of optically polished graphite produces images with a high frequency of high-value pixel intensities. Pores exposed to the surface are less reflective and appear as grey (or dark) objects with low-value pixel intensities. The roughness of graphite surface increases in the layer penetrated by oxidation, which results in images with higher population of low-value pixel intensities. Histogram analysis of images allowed consistent identification of pores and visual segmentation of images. Based on analysis of many images, the changes introduced by oxidation were identified as new peaks (or shoulders) on intensity histograms at pixel values below the median level (Fig. 1). Next, visual images of objects (pores) were extracted, their properties were measured, and the objects were classified based on size, area, perimeter, aspect ratio, clustering, etc. In particular, profile analysis of pixel intensities distribution along the specimen's diameter allowed characterizing the position of oxidation-induced pores relative to the exposed surface of specimens (Fig. 2).

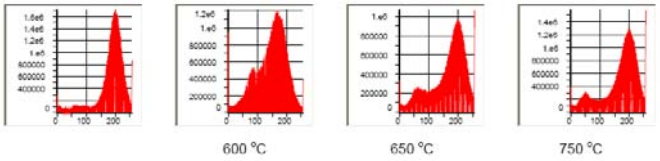

Fig. 1: Intensity histograms of pristine and oxidized graphite specimens (20 %weight loss at various temperatures).

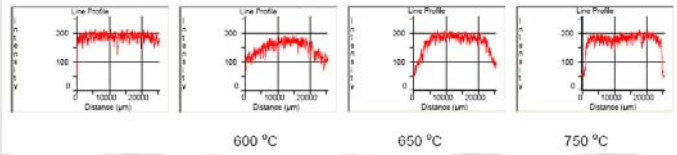

Fig. 2: Profile analysis of pixel intensity distribution along a specimen's diameter (25.4 mm) for pristine and oxidized graphite (20% weight loss at various temperatures).

Results

Mosaic pictures in Fig. 3 consist of 216 individual images taken at 200x magnification. The pictures show penetration of the oxidized layer in a region about 13 mm deep from the exposed surface (on left). In this example the weight loss after oxidation was 5 % at temperatures between 600 and 750 ^{o}C. The pores were classified based on their area in two classes. The pictures show that the thickness of the oxidized layer depends strongly on oxidation temperature. At low temperatures (e.g 600 ^{o}C) oxidation is in the chemical (or kinetic) regime, where the rate of chemical reaction is slow compared with the rate of diffusion of the oxidant in the bulk. With the increase of oxidation temperature, the rate of chemical reaction increases faster than that of in-pore diffusion, and the mechanism shifts to pore-diffusion control. As temperature increases even more (e.g. at 750 ^{o}C) oxidation is limited to a narrow layer near the surface. At these high temperatures, however, the bulk of the specimens is not modified significantly, as shown by comparing the distribution

of porosity in the pristine specimen and the bulk of specimen oxidized at 750 °C (Fig. 3).

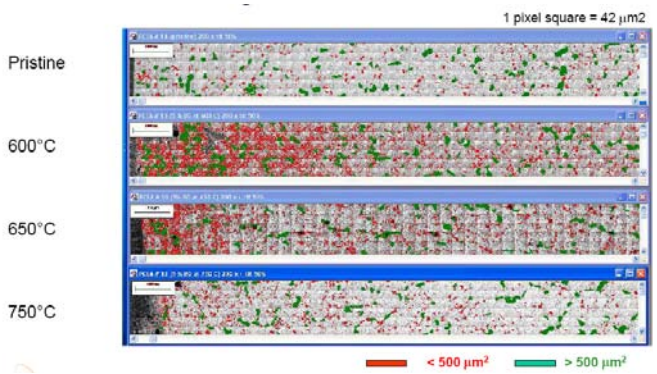

Fig. 3: Progress of oxidized layer with temperature (5 % net weight loss). Mosaic images cover the radius of specimens from surface (left) to center (right). Scale bar = 1 mm.

Discussion

Gas-solid reactions are the net result of two concurrent processes whose rates have a very different variation with temperature: The rate of chemical oxidation increases much faster with temperature than the effective diffusivity of the oxidant in the porous structure of graphite. This fact causes transition between regime 1 (kinetic control) and regime 2 (in-pore diffusion control) of oxidation, usually reported as a change of slope in the Arrhenius representation of oxidation rates [3]. Interestingly, the Arrhenius plot of oxidation rates for the examples analyzed here was perfectly linear (Fig. 4) although the oxidation profile was clearly not uniform (Fig. 3). This shows that the linearity of Arrhenius plot does not necessary confirm that oxidation is uniform in the bulk of specimens [4].

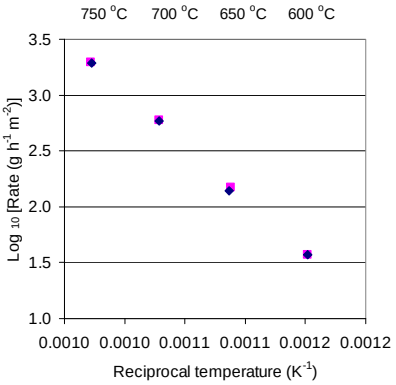

Fig. 4: Arrhenius plots of oxidation rates

Fig. 5 shows the development of porosity at constant temperature (600 °C) with the level of weight loss. In this example the pores have been classified in 10 classes based on area. It seen that the depth of the oxidized layer is almost constant (in this example, about 6 mm). From this and other examples it was concluded that the penetration depth of the oxidant is a strong function of temperature, as predicted [5] by previous model calculations and also found experimentally [4]. Close examination of images at higher magnification showed that the most important effect of oxidation on microstructure consists in development of narrow, slit-shaped pores located mostly in the binder phase between graphitized coke particles [6]. These pores multiply dramatically with the increase of burn-off level at constant temperature, and eventually collapse into larger pores (Fig. 5).

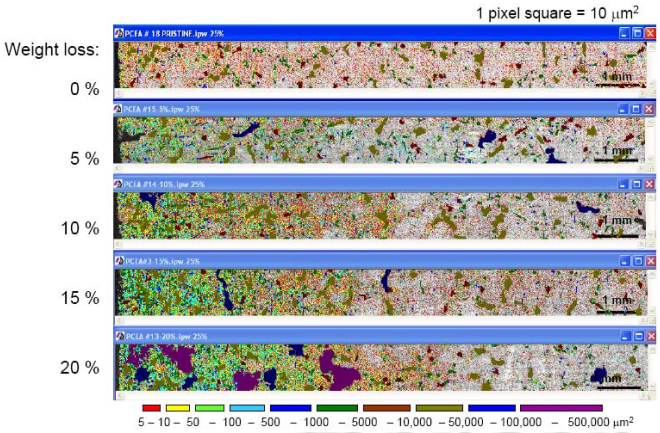

Fig. 5: Development of porosity in the oxidized layer with the level of weight loss at 600 °C. Scale bar = 1 mm.

Conclusions

Optical microscopy enhanced by automated image analysis is a valuable tool for characterizing porosity development in oxidized graphite. The method is quick, affordable, convenient, and provides statistical information on pore distribution. The method has the potential to provide microstructural information needed for better understanding and modeling of graphite oxidation effects on structural integrity and mechanical properties.

Acknowledgments: Research supported by Division of Nuclear Energy, U.S. Department of Energy, under NGNP Program. Oak Ridge National Laboratory is managed by U.T. Battelle LLC under contract DE-AC05-00OR22275.

References

[1] Babout L, Mummery PM, Marrow TJ, Tzelepi A, Withers PJ. The effect of thermal oxidation on polycrystalline graphite studied by X-ray tomography, Carbon 2005; 43: 765-774.
[2] Chi S-H, Burchell TD, Contescu CI. Density change of an oxidized nuclear graphite by acoustic microscopy and image processing. J Eng Gas Turbines Power 2009; 131: 052904.
[3] Fuller EL, Okoh JM. Kinetics and mechanisms of the reaction of air with nuclear grade graphites: IG-110, J Nucl Mater 1997; 240: 241-250.
[4] Contescu CI, Azad S, Miller D, Lance MJ, Baker FS. Practical aspects for characterizing air oxidation of graphite, J Nucl Mater 2008; 381: 15-24.
[5] Wichner RP, Burchell TD, Contescu CI. Penetration depth and transient oxidation of graphite by oxygen and water vapor, J Nucl Mater 2009; 393: 518-521.
[6] Pickup IM, McEnaney B, Cooke RG. Fracture processes in graphite and the effects of oxidation, Carbon 1986; 24: 535-543.